Hydrological Persistence and the Hurst Phenomenon (SW-434)

Demetris Koutsoyiannis

Department of Water Resources, Faculty of Civil Engineering, National Technical University, Athens,
Heroon Polytechneiou 5, GR-157 80 Zographou, Greece (dk@itia.ntua.gr)

Abstract Unlike common random series like those observed for example in games of chance, hydrological (and other geophysical) time series have some structure, that is, consecutive values of hydrological time series are dependent to each other. A special kind of dependence observed at large timescales has been discovered by Hurst half a century ago and has been known by several names such as long-range dependence, long-term persistence or simply the Hurst phenomenon. Since then, it has been verified that this behaviour is almost omnipresent in several processes in nature (e.g. hydrology), technology (e.g. computer networks) and society (e.g. economics). The consequences of this behaviour are very significant, as it increases dramatically the uncertainty of the related processes. However, even today its importance and its consequences are not widely understood or are ignored, its nature is regarded as difficult to understand, and its reproduction in hydrological simulation is considered a hard task or not necessary. It is shown in this article that the Hurst phenomenon can have easy explanation and easy stochastic representation, and that simple algorithms can generate time series exhibiting long-term persistence.

Introduction

Unlike common random series like those observed for example in games of chance (dice, roulette, etc.), hydrological (and other geophysical) time series have some structure, that is, consecutive values of hydrological time series are dependent to each other. It is easy to understand that, for instance in a monthly river flow series, a month with very high flow is

likely to be followed by a month with high flow, too. Since the river flow is interrelated to the groundwater storage, the high flow indicates that the groundwater storage will be high too, and given that the groundwater flow is a slow process, it is expected that its contribution to the river flow in the next month will be significant. This explains the dependence of consecutive values of hydrological time series, which has been known as *short-range* (or *short-term*) *dependence, persistence, or memory.*

Interestingly, however, there is another kind of dependence observed at larger timescales, known as *long-range* (or *long-term*) *dependence, persistence, or memory*. This has been discovered by Hurst (1951), while investigating the discharge time series of the Nile River in the framework of the design of the Aswan High Dam, and found in many other hydrological and geophysical time series. This behaviour is essentially the tendency of wet years to cluster into multi-year wet periods or of dry years to cluster into multi-year drought periods. The terms 'Hurst phenomenon' and 'Joseph effect' (due to Mandelbrot, 1977, from the biblical story of the 'seven years of great abundance' and the 'seven years of famine') have been used as alternative names for the same behaviour. Since its original discovery, the Hurst phenomenon has been verified in several environmental quantities such as (to mention a few of the more recent studies) in wind power (Haslett and Raftery, 1989); global or point mean temperatures (Bloomfield, 1992; Koutsoyiannis, 2003a, b); flows of several rivers such as Nile (Eltahir, 1996; Koutsoyiannis, 2002), Warta, Poland (Radziejewski and Kundzewicz, 1997), Boeoticos Kephisos, Greece (Koutsoyiannis, 2003a), and Nemunas, Lithuania (Sakalauskienė, 2003); inflows of Lake Maggiore, Italy (Montanari et al., 1997); indexes of North Atlantic Oscillation (Stephenson et al., 2000); and tree-ring widths, which are indicators of past climate (Koutsoyiannis, 2002). In addition, the Hurst phenomenon has gained new interest today due to its relation to climate changes (e.g. Evans, 1996; Koutsoyiannis, 2003a, c; Koutsoyiannis and Efstratiadis, 2004).

The possible explanation of the long-term persistence must be different from that of the short-term persistence discussed above. This will be discussed later. However, its existence is easy to observe even in a time series plot, provided that the time series is long enough. For example, in Figure 1 (up) we have plotted one of the most well-studied time series, that of the

annual minimum water level of the Nile river for the years 622 to 1284 A.D. (663 observations), measured at the Roda Nilometer near Cairo (Toussoun, 1925, p. 366-385; Beran, 1994). In addition to the plot of the annual data values versus time, the 5-year and 25-year averages are also plotted versus time. For comparison we have also plotted in the lower panel of Figure 1 a series of white noise (consecutive independent identically distributed random variates) with statistics same with those of the Nilometer data series. We can observe that the fluctuations of the aggregated processes, especially for the 25-year average, are much greater in the real world time series than in the white noise series. Thus, the existence of fluctuations in a time series at large scales distinguishes it from random noise.
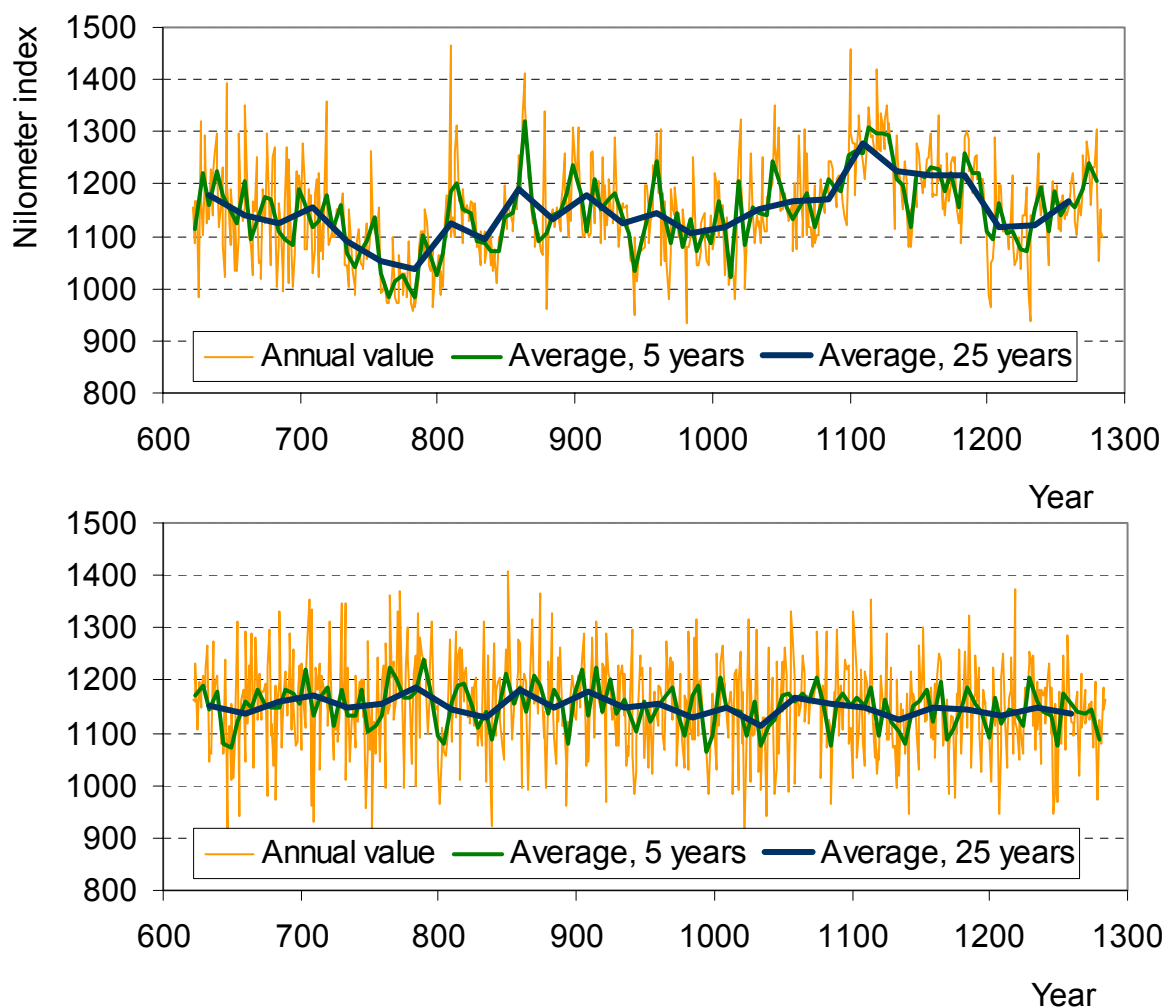
Figure 1 (Up) Plot of the Nilometer series indicating the annual minimum water level of the Nile River for the years 622 to 1284 A.D. (663 years); (down) a white noise series with same mean and standard deviation, for comparison.

Stochastic representation of the Hurst phenomenon

The quantification of the long-term persistence is better expressed mathematically using the theory of stochastic processes. Let X_i denote a stochastic representation of a hydrometeorological process with $i = 1, 2, \ldots$, denoting discrete time with time step or scale which for the purposes of this article is annual or multi-annual. It is assumed that the process is stationary, a property that does not hinder to exhibit multiple scale variability. The stationarity assumption implies that its statistics are not functions of time. Therefore, we can denote its statistics without reference to time, i.e. its mean as $\mu := E[X_i]$, its autocovariance as $\gamma_j := \text{Cov}[X_i, X_{i+j}]$ ($j = 0, \pm1, \pm2, \ldots$), its autocorrelation $\rho_j := \text{Corr}[X_i, X_{i+j}] = \gamma_j / \gamma_0$, and its standard deviation $\sigma := \sqrt{\gamma_0}$. Further, we assume ergodicity, so that these statistics can be estimated from a unique time series substituting time averages for expected values.

Let k be a positive integer that represents a timescale larger than the basic timescale of the process X_i. The aggregated stochastic process on that timescale is denoted as

$$Z_i^{(k)} := \sum_{l=(i-1)k+1}^{ik} X_l \tag{1}$$

The statistical characteristics of $Z_i^{(k)}$ for any timescale k can be derived from those of X_i. For example, the mean is

$$E[Z_i^{(k)}] = k\,\mu \tag{2}$$

whilst the variance and autocovariance (or autocorrelation) depends on the specific structure of γ_j (or ρ_j). In a process that exhibits the Hurst phenomenon, the variance $\gamma_0^{(k)}$ for timescale k is related to that of the basic scale γ_0 by

$$\gamma_0^{(k)} := \text{Var}[Z_i^{(k)}] = k^{2H}\,\gamma_0 \tag{3}$$

where H is a constant known as the Hurst coefficient with values in the interval (0.5, 1). The value $H = 0.5$ corresponds to random noise whereas values in the interval (0, 0.5) are mathematically possible but without interest in hydrology. Consequently, the standard deviation is a power law of the scale or level of aggregation k with exponent H, i.e.,

$$\sigma^{(k)} := \left(\gamma_0^{(k)}\right)^{1/2} = k^H \sigma \tag{4}$$

This simple power law can be easily used both for detecting whether a time series exhibits the Hurst phenomenon and for determining the coefficient H, which is a measure of the long-term persistence. Equation (4) calls for a double logarithmic plot of standard deviation $\sigma^{(k)}$ of the aggregated process $Z_i^{(k)}$ versus timescale k. In such a plot, called the aggregated standard deviation plot, the Hurst behaviour is manifested as a straight line arrangement of points corresponding to different timescales, whose slope is the Hurst coefficient. An example is depicted in Figure 2 for the Nilometer series of Figure 1. Clearly, the plot of the empirical estimates of standard deviation is almost a straight line on the logarithmic diagram with slope 0.85. For comparison we have also plotted the theoretical curve for the white noise with slope equal to 0.5, significantly departing from the historical data.
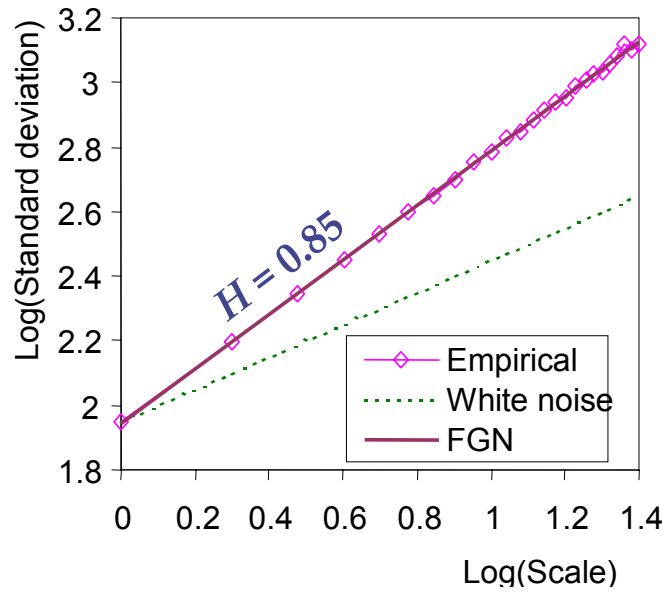
Figure 2 Aggregated standard deviation plot of the Nilometer series.

By virtue of (3), it can be shown that the autocorrelation function, for any aggregated timescale k, is independent of k and given by

$$\rho_j^{(k)} = \rho_j = (1 / 2)\,(|j + 1|^{2H} + |j - 1|^{2H}) - |j|^{2H}) \approx H\,(2\,H - 1)\,|j|^{2H - 2} \tag{5}$$

which shows that autocorrelation is a power function of lag. Consequently, the autocovariance $\gamma_j^{(k)} = \gamma_0^{(k)}\,\rho_j^{(k)}$ is a power law of both the scale k (with exponent $2H$) and the lag j (with exponent $2H - 2$).

The power spectrum of the process

$$s_\gamma^{(k)}(\omega) := 2 \sum_{j=-\infty}^{\infty} \gamma_j^{(k)} \cos (2\pi j\,\omega) \tag{6}$$

is given approximately by

$$s_\gamma^{(k)}(\omega) \approx 4\,(1-H)\,\gamma_0^{(k)}\,(2\,\omega)^{1-2H} \tag{7}$$

which is a power law of both the scale k (with exponent $2H$) and the frequency ω (with exponent $1-2H$).

The power law equations (5) and (7) can be used, in addition or alternatively to (3) and (4), to detect the Hurst behaviour of a time series. It should be mentioned here that Hurst's (1951) original formulation to detect this behaviour was based on another quantity, the so called rescaled range, which corresponds to the cumulated process of inflow minus outflow of a hypothetical infinite reservoir.

Equations (3)-(7) describe essentially second order properties of the process $Z_i^{(k)}$. A generalization is possible, if we assume that the process of interest exhibits scale invariant properties in its (finite dimensional joint) distribution function, i.e.,

$$(Z_i^{(k)} - k\,\mu) \overset{\mathrm{d}}{=} \left(\frac{k}{l}\right)^{H} (Z_j^{(l)} - l\,\mu) \tag{8}$$

where the symbol $\overset{\mathrm{d}}{=}$ stands for equality in distribution. In this case, (3) can be obtained from (8) setting $i = j = l = 1$ and taking the variance of both sides. Equation (8) defines X_i and $Z_i^{(k)}$ as stationary increments of a self-similar process. If, in addition, X_i (and hence $Z_i^{(k)}$) follows the normal distribution, then X_i (and $Z_i^{(k)}$) is called fractional Gaussian noise (FGN; Mandelbrot, 1965). Our interest here includes processes that may be not Gaussian, so we will limit the scaling property (8) to second-order properties only and call the related process a *simple scaling signal* (SSS).

Physical explanations of the Hurst phenomenon

As described in the Introduction, the concept of short-term persistence in hydrological processes is ease to explain, whereas long-term persistence and the Hurst phenomenon are more difficult to understand. Mesa and Poveda (1993) classify the Hurst phenomenon as one

of the most important unsolved problems in hydrology and state that "something quite dramatic must be happening from a physical point of view". However, several explanations have been proposed. These can be classified in two categories: physically-based and conceptual.

Klemeš (1974) proposed an explanation that may be classified in the first category. According to this, the Hurst behaviour of hydrological records can be explained by representing the hydrological cycle by a 'circular cascade of semi-infinite storage reservoirs' where the output from one reservoir constitutes an essential part of input into the next. He showed that, even with an originally uncorrelated Gaussian forcing, the outputs grew progressively more Hurst-like with an increasing complexity of the system, e.g. with the number of reservoirs in the cascade. Another example of such hydrological system was suggested in Klemeš (1978).

Beran (1994, pp. 16-20) describes two physically-based model types that lead to system evolution (in time or space) with long-range dependence. The first model type applies to critical phenomena in nature such as phase transition (transition from liquid to gaseous phase, or spontaneous magnetization of ferromagnetic substances). For some critical system temperature the correlation of the system state at any two points decays slowly to zero, so the correlation in space can be represented by (5). The second type is related to models based on stochastic partial differential equations, which, under certain conditions, result in solutions with long-range dependence. These models provide sound links of long-range dependence with physics but are very complex.

A simple model of this category was studied by Koutsoyiannis (2003b). This model assumes a system with purely deterministic dynamics in discrete time, which however results in time series with irregular appearance exhibiting the Hurst phenomenon. The system dynamics is based on the simple map

$$x_i = g(x_{i-1}; \alpha) := \frac{(2-\alpha)\,\min\,(x_{i-1},\,1-x_{i-1})}{1-\alpha\,\,\min\,(x_{i-1},\,1-x_{i-1})} \tag{9}$$

where x_i is the system state, assumed to be scalar, at time i and $\alpha < 2$ is a parameter. This map, known as generalized tent map, has been used in the study of dynamical systems. For

example, the map approximates the relation between successive maxima in the variable $x(t)$ from the Lorenz equations that describe climatic dynamics (Lasota and Mackey, 1994, p. 150). Koutsoyiannis (2003b) demonstrated that this model can describe a system subject to the combined action of a positive and a negative feedback. If the parameter α is assumed to vary in time following the same map, i.e., $\alpha_i = g(\alpha_{i-1}; \lambda)$, then we obtain the double tent map

$$u_i = G(u_{i-1}, \alpha_{i-1}; \kappa, \lambda) := g(u_{i-1}; \kappa \, \alpha_{i-1}) \tag{10}$$

Both parameters κ and λ should be < 2 whereas the domain of u_t is the interval [0, 1]. If the system domain is the entire line of real numbers, we can apply an additional transformation to shift from [0, 1] to $(-\infty, \infty)$, e.g.,

$$x_t = \ln[u_t / (1 - u_t)] \tag{11}$$
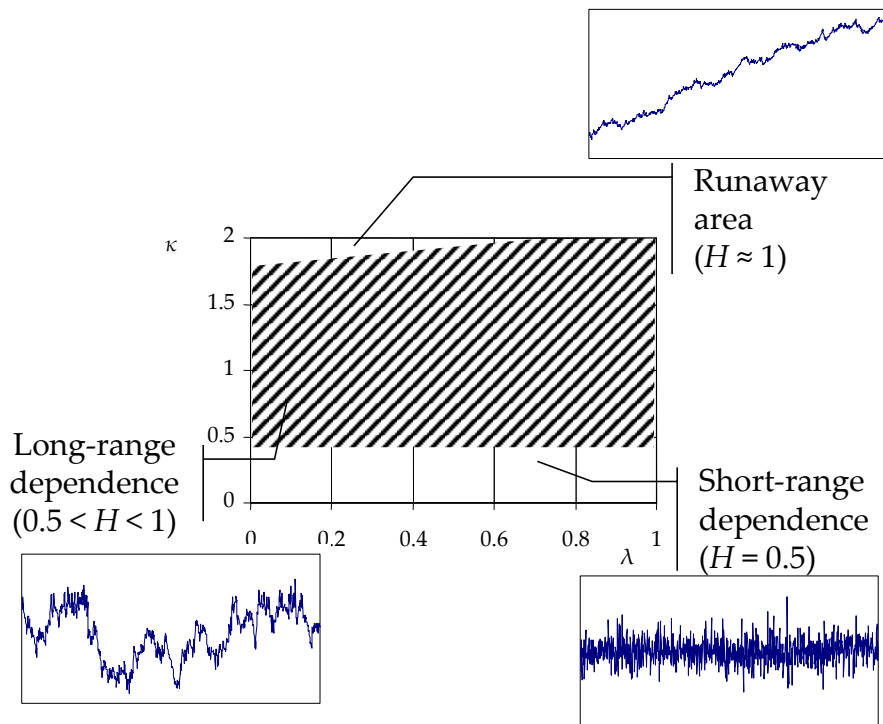
Figure 3 Schematic of the general behaviour of the double tent map in terms of the ranges of its parameters κ and λ.

The model behaviour with respect to parameters κ and λ is depicted in Figure 3. We observe that for small values of the parameter κ, the time series synthesized by the model exhibit short-range dependence with Hurst coefficient around 0.5. For large values of κ, the

model yields a runaway behaviour. However, in between the two non-interesting areas, there is an area of parameter values, shaded in Figure 3, in which the resulting time series exhibit the long-range dependence. All three types of behaviour are observed for negative values of λ (not shown in Figure 3) whereas for $\lambda > 1$ only the runaway behaviour is observed regardless of the value of κ.

The second category, labelled here 'conceptual', does not aim at explaining the physical mechanism leading to Hurst behaviour of historical records of some natural or other processes, but examines different stochastic mechanisms that might produce realizations resembling the patterns of the observed empirical time series. For example, Klemeš (1974) analyzed several variants of the 'changing mean' mechanism which assumes that the mean of the process is not a constant determined by the arithmetic mean of the record, but varies through time. Specifically, he performed numerical experiments with the following Gaussian random processes:

1. a process with the mean alternating periodically between two values after constant time intervals called 'epochs';

2. a process with a monotonic linear trend in the mean, throughout the entire series length;

3. a process similar to 1 but with epoch lengths taking two different values with probabilities p and $1 - p$; and

4. a process with a Gaussian-distributed mean randomly varying from epoch to epoch, the epoch length also varying randomly and following either a uniform, exponential, or (single parameter) Pareto distribution.

The processes behaved increasingly Hurst-like as their structure changed from 1 to 4. This behaviour was most influenced by the distribution of epoch lengths, while the distribution of the mean itself had little effect.

The effect of periodical patterns, which are extensions of those of model 1, have been thoroughly studied by Montanari et al. (1999), who however note that such patterns are unusual in real data. The effect of monotonic deterministic trends, which are extensions of

model 2, was studied by Bhattachara et al. (1983), who showed mathematically that a trend of the form $f(t) = c\,(m + t)^{H-1}$ with t denoting time, c a nonzero constant, m a positive constant and H a constant in the interval (0.5, 1), results in time series exhibiting the Hurst phenomenon with Hurst coefficient precisely equal to H. We may note, however, that this kind of nonstationarity with a monotonic deterministic trend spanning the whole length of a time series can hardly represent a long time series of real data, even though in short time series seem to be realistic. For example, to refer to the Nilometer series of Figure 1, if one had available only the data of the period 700-800 one would detect a 'deterministic' falling trend of the Nile level; similarly, one would detect a regular rising trend of the Nile level between the years 1000-1100. However, the complete picture of the series suggests that these trends are parts of large-scale random fluctuations rather than deterministic trends.

Based on this observation, Koutsoyiannis (2002) proposed a conceptual explanation, which can be essentially regarded as an extension of Klemeš's model 4 and is also similar to other proposed conceptual models as it will be discussed later. More specifically, Koutsoyiannis (2002) demonstrated that superimposition of three processes with short-term persistence results in a composite process that is practically indistinguishable from an SSS process.

This demonstration is reproduced here in Figures 4-5. It starts assuming a Markovian process U_i, like the one graphically demonstrated in Figure 4(a), with mean $\mu := E[U_i]$, variance γ_0 and lag one autocorrelation coefficient $\rho = 0.20$. The specific form of this process is an AR(1) one, i.e. $U_i := \rho\,U_{i-1} + E_i$, where E_i is white noise, and its autocorrelation is

$$\text{Corr}[U_i, U_{i+j}] = \rho^j \tag{12}$$

The autocorrelation function is shown in Figure 5(a) along with the autocorrelation function of SSS with same lag one autocorrelation coefficient (0.20). We observe the large difference of the two autocorrelation functions: that of the Markovian process practically vanishes off at lag 4 whereas that of SSS has positive values for lags as high as 100.

In the next step, a second process V_i is constructed by superimposing another Markovian process M_i, i.e.,

$$V_i = U_i + M_i - \mu \tag{13}$$

Here the process M_i is constructed in a different way, rather than using the AR(1) model, yet without loosing its Markovian behaviour, so that its autocorrelation is

$$\text{Corr}[M_i, M_{i+j}] = \varphi^j \qquad (14)$$

for $\varphi > \rho$. More specifically, a continuous time process M (see explanatory sketch on Figure 4(b)) with the following properties was assumed: (a) it has mean μ and some variance $\text{Var}[M]$; (b) any realization m of M lasts N years and is independent from previous realizations; (c) N is a random variable exponentially distributed with mean $\lambda = -1 / \ln \varphi$. (This means that N can take non-integer values). In other words, M takes a value $m_{(1)}$ that lasts n_1 years, then it changes to a value $m_{(2)}$ that lasts n_2 years, etc. (where the values $m_{(1)}$, $m_{(2)}$, … can be generated from any distribution). The exponential distribution of N indicates that the points of change are random points in time. If we denote M_i the instance of the M process at discrete time i, it can be shown that indeed M_i is Markovian with lag one autocorrelation φ. This way of constructing M_i allows us to interpret V_i as a process similar to U_i but with mean M_i that varies randomly in time (rather than being constant, μ) shifting among randomly determined values $m_{(1)}$, $m_{(2), …}$, each lasting a random time period with average λ. It can be easily shown from (13) that the autocorrelation of V_i for lag j is

$$\text{Corr}[V_i, V_{i+j}] = (1 - c)\rho^j + c \, \varphi^j \qquad (15)$$

where $c := \text{Var}[M_i] / (\text{Var}[M_i] + \text{Var}[U_i])$. Setting for instance $\lambda = 7.5$ years ($\varphi = 0.875$) and $c = 0.146$ we get the autocorrelation function shown in Figure 5(b), which has departed from the AR(1) autocorrelation and approached the SSS autocorrelation.

In a third step, another process W_i is constructed by superimposing V_i with a third Markovian process P_i, i.e.,

$$W_i = V_i + P_i - \mu = U_i + M_i + P_i - 2\mu \qquad (16)$$

P_i is constructed in a way identical to that of M_i, but with lag one autocorrelation $\xi > \varphi$, so that the mean time between changes of the value of P is $v = -1 / \ln \xi$. Working as in the previous step we find

$$\text{Corr}[W_i, W_{i+j}] = (1 - c_1 - c_2)\rho^j + c_1 \, \varphi^j + c_2 \, \xi^j \qquad (17)$$

where c_1 and c_2 are positive constants (with $c_1 + c_2 < 1$). Setting for instance $\lambda = 7.5$ years ($\varphi = 0.875$), $v = 200$ years ($\xi = 0.995$), $c_1 = 0.146$ and $c_2 = 0.036$ we get the autocorrelation function shown in Figure 5(c), which has now become almost indistinguishable from the SSS autocorrelation for time lags from 1 to 1000.
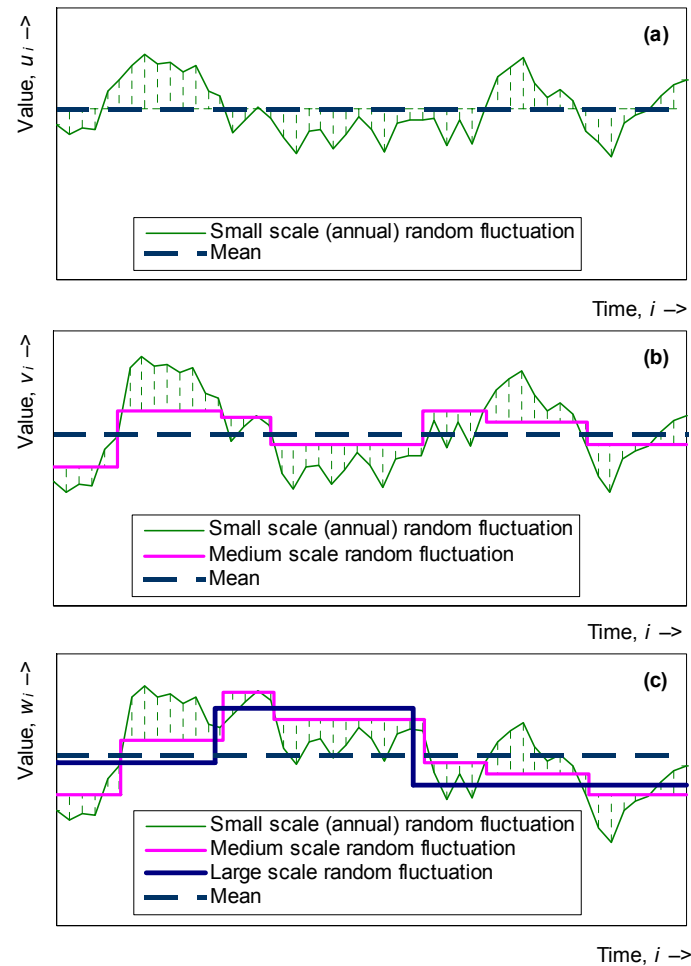
Figure 4 Illustrative sketch for multiple timescale random fluctuations of a process that can explain the Hurst phenomenon: (a) a time series from a Markovian process with constant mean; (b) the same time series superimposed to a randomly fluctuating mean on a medium timescale; (c) the same time series further superimposed to a randomly fluctuating mean on a large timescale (from Koutsoyiannis, 2002).

In conclusion, a Markovian underlying process can result in a nearly SSS process if there occur random fluctuations of the mean of the process on two different scales (e.g., 7.5 and 200 years), yet the resulting composite process being stationary. If we consider that fluctuations occur on a greater number of timescales, the degree of approximation of the

composite process to the SSS process will be even better and can cover time lags greater than 1000 (although the extension to lags beyond 1000 may not have any practical interest in hydrology). In conclusion, the *irregular* changes of climate that, according to National Research Council (1991, p. 21), occur on all timescales can be responsible for, and explain, the Hurst phenomenon.
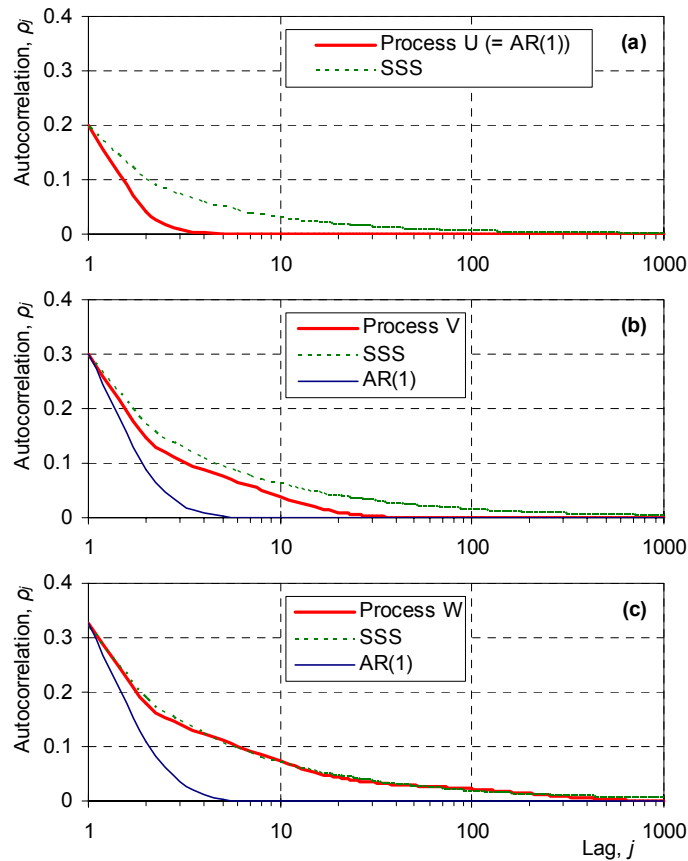
Figure 5 Plots of the example autocorrelation functions of (a) the Markovian process U with constant mean; (b) the process U superimposed to a randomly fluctuating mean on a medium timescale (process V); (c) the process V further superimposed to a randomly fluctuating mean on a large timescale (process W). The superimposition of fluctuating means increases the lag one autocorrelation (from $\rho_1 = 0.20$ for U to $\rho_1 = 0.30$ and 0.33 for V and W respectively) and also shifts the autocorrelation function from the AR(1) shape (also plotted in all three panels) towards the SSS shape (also shown in all three panels) (from Koutsoyiannis, 2002).

This demonstration, in fact bridges several ideas that had been proposed to explain the Hurst phenomenon, rather than being a novel explanation. As already discussed, it is similar with Klemeš's model 4, except for the setting of multiple timescales of fluctuation of mean

and the emphasis on the stationarity of the composite process. Here, it should be mentioned that Klemeš referred to all his 'changing mean' models as models with nonstationarity in their mean, even though this is strictly true only for models 1 and 2. While he did point out that his final models in group 4 were in fact stationary, and that he kept the term 'nonstationary' for all changes in the mean to communicate the fact (elaborated in more detail in Klemeš, 1976) that one cannot tell the difference from the pattern of a single 'nonstationary-looking' time series (which even a stationary model is designed to mimic), his explanation has sometimes been missed and lead to a misconception about his work by some authors (including this one, who expresses his apology).

The idea of irregular sporadic changes in the mean of the process appeared also in Salas and Boes (1980), but not in connection with SSS and not in the setting of multiple timescales. The idea of composite random processes with two timescales of fluctuation appeared in Vanmarcke (1983, p. 225). The idea of an explanation of the Hurst phenomenon as a mixture of scales appears in Mesa and Poveda (1993). The idea of representing SSS as an aggregation of short-memory processes is the principle of the well known fast fractional Gaussian noise algorithm (FFGN, Mandelbrot, 1971) and is also studied, as a possible physical explanation of the Hurst phenomenon, by Beran (1994, p. 14). The difference of the above described explanation is the aggregation of only three short-memory processes.

Importance of the Hurst phenomenon

The presence of the Hurst phenomenon increases dramatically the uncertainty of climatic and hydrological processes. If such a process were random and our information on this was based on a sample of size n, then the uncertainty on the long term, which can be expressed in terms of the variance of the estimator of the mean, $\overline{X}$, would be:

$$\mathrm{var}[\overline{X}] = \frac{\sigma^2}{n} \tag{18}$$

This offers good approximation for a process with short-term persistence, as well, but it is not valid for a process with long-term persistence. Instead, the following relation holds (Adenstedt, 1974; Beran, 1994, p. 54; Koutsoyiannis, 2003a):

$$\mathrm{var}[\bar{X}] = \frac{\sigma^2}{n^{2-2H}} \tag{19}$$

The difference between equations (18) and (19) becomes very significant for large values of *H*. For example, in a time series of $n = 100$ years of observations and standard deviation σ, according to the classical statistics (equation (18)), the standard estimation error, i.e. the square root of $\mathrm{var}[\bar{X}]$, is $\sigma/10$. However, for $H = 0.8$ the correct standard error, as given by equation (19), is $\sigma/2.5$, i.e. four times larger. To have an estimation error equal to $\sigma/10$, the required length of the time series would be 100 000 years! Obviously, this dramatic difference induces substantial differences in other common statistics as well (Koutsoyiannis, 2003a).

A demonstration of the difference in estimations related to climate is given in Figure 6. Here, a long climatic time series (992 years) was used, which represents the Northern Hemisphere temperature anomalies with reference to 1961–1990 mean (Figure 8, up) This series was constructed using temperature sensitive palaeoclimatic multi-proxy data from 10 sites worldwide that include tree rings, ice cores, corals, and historical documents (Jones et al., 1998a, b). The time series was studied in relation to the Hurst phenomenon by Koutsoyiannis (2003a) and it was found that the estimate of the Hurst coefficient is 0.88. In the upper panel of Figure 6 the point estimates and the 99% confidence limits of the quantiles of the temperature anomalies have been plotted for probability of nonexceedence, *u*, ranging from 1 to 99%, assuming a normal distribution, as verified from the time series, and using the classical statistical estimators. This is done for two timescales, the basic one ($k = 1$) that represents the annual variation of temperature anomaly, and the 30-year timescale, which typically is assumed to be sufficient to smooth out the annual variations and provide values representative of the climate. (For the latter, the averaged rather than aggregated time series, i.e. $z_i^{(30)}/30$, has been used.)
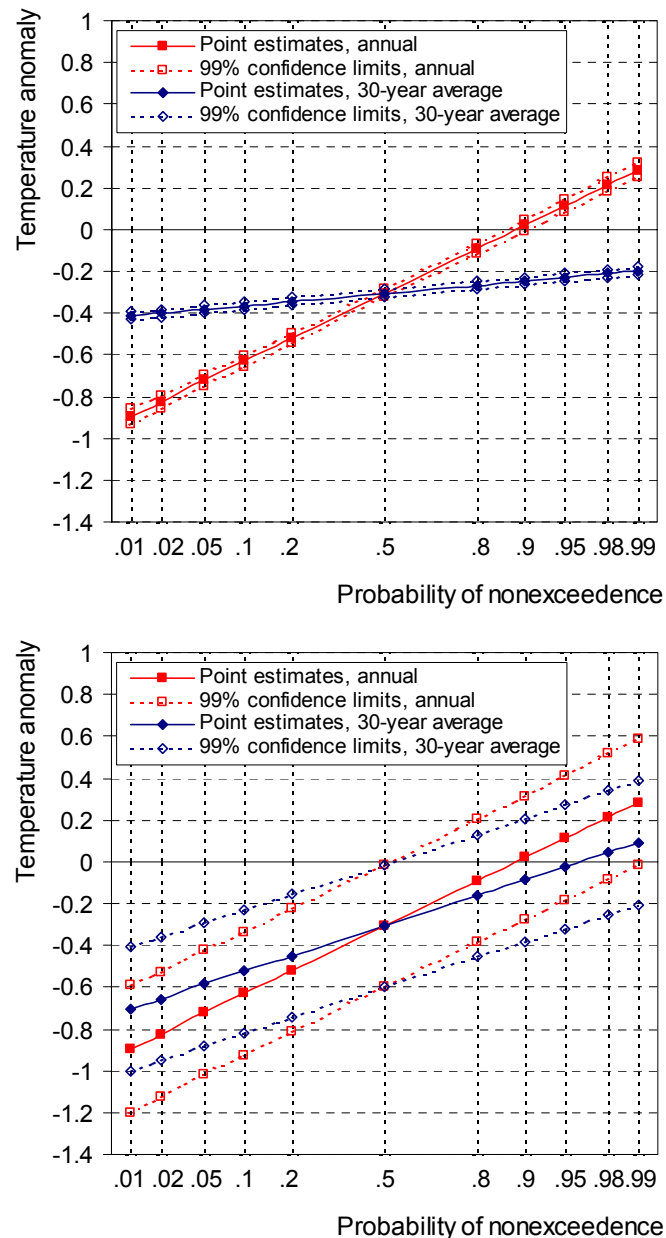
Figure 6 Point estimates of quantiles and 99% confidence limits thereof at the basic timescale (annual values, *k* = 1) and the 30-year timescale (30-year averages, *k* = 30), for the Jones's time series of the Northern Hemisphere temperature anomalies: (up) using classical statistics; (down) using adapted statistics.

If classical statistics is used (Figure 6, upper panel), then it is observed that, due to the large length of the series, the confidence band is very narrow and the point estimates for the basic and the aggregated timescale differ significantly. The variability of climate, as expressed by the distribution of the average at the 30-year timescale, is very low, despite the much higher variability at the annual scale. This justifies the saying "Climate is what you

expect, weather is what you get". Things change dramatically, if the statistics based on the hypothesis of long-term persistence (Koutsoyiannis, 2003a) are used with $H = 0.88$. This is depicted in the lower panel of Figure 6, where it is observed that the variation of the 30-year average is only slightly lower than that of the annual values and the confidence band has dramatically widened for both timescales. This could be expressed by paraphrasing the above proverb to read "Weather is what you get, climate is what you get – if you keep expecting for many years". The consequences of these differences in estimating the climatic uncertainty due to natural variability are obviously very significant.

The consequences in the water resources engineering and management are even more significant. Particularly, since the notion of climate implies long timescales, it is to be expected that the practical importance of the Hurst phenomenon increases in projects whose operation cycles span across long periods of time. As a typical example may serve large reservoirs with multi-year flow regulation (Klemeš et al., 1981; see also the entry SW-776, Reliability Concepts in Reservoir Design). For small-to-middle range reservoirs it is generally regarded that the effect of the Hurst phenomenon appears to be within the margin of error of hydrological data used for their design and operation. However, even in hydrosystems with small reservoirs or no reservoirs at all, as it becomes obvious from the above discussion, the effect on the Hurst phenomenon is significant if the uncertainty (not only the expected value) of water availability is to be assessed.

Simple algorithms to generate time series respecting the Hurst phenomenon

Several algorithms have been developed to generate time series that respect the Hurst phenomenon. Among these, we discuss here the simplest ones that can be applied even in a spreadsheet environment. These are based on the above-discussed properties of SSS and can be used to provide approximations of SSS good for practical hydrological purposes.

A first, rather "quick and dirty" algorithm can be very easily formulated based on the deterministic double tent map (equations (10) and (11)). The problem with the resulting time series is that consecutive generated values are too regularly and smoothly related. This can be avoided by discarding some of the generated values x_i and holding only the values x_{vj}, for

some $v > 1$ and for $j = 1, 2, …, n$, where n is the required series length. Figure 7 depicts the attained Hurst coefficient in a time series generated from the double tent map (equation (10)) either untransformed or transformed (equation (11)) for $v = 1$ and 4. This figure can serve as a tool to estimate the parameter κ required to achieve a certain Hurst coefficient H (assuming $\lambda = 0.001$). A time series so generated can then be transformed linearly to acquire the required mean and standard deviation. By appropriately choosing the initial values α_0 and u_0 one can obtain a time series that can have a presumed general shape; this needs a random search optimization technique to be applied. An example of the application of this algorithm to the Jones data set already discussed above is depicted in Figure 8.
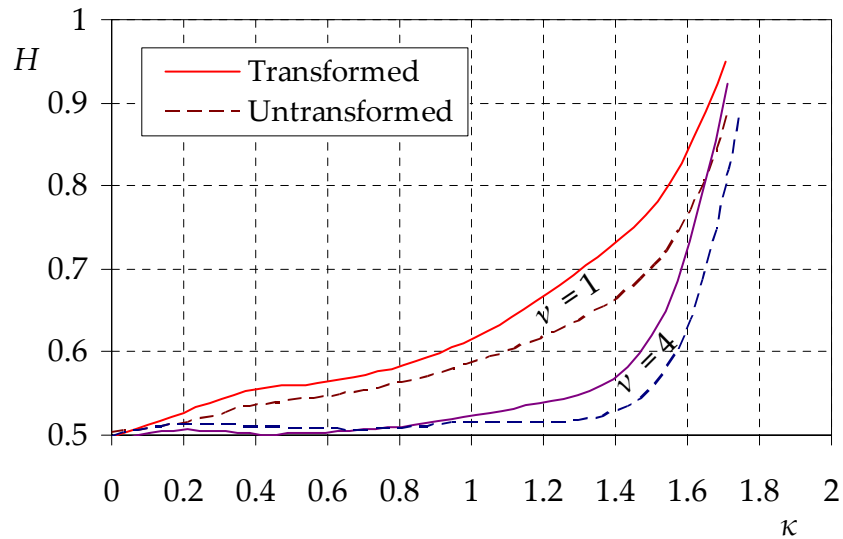

Figure 7 Hurst coefficient of a time series generated from the double tent map (equations (10) and (11)) for parameter values $\lambda = 0.001$, κ ranging from 0 to 2 and $v = 1$ and 4. For κ approaching 2 the double tent map has a runaway behaviour.

As we saw earlier, the weighted sum of three exponential functions of the time lag (equation (17)) can give an acceptable approximation of the SSS autocorrelation function on the basic timescale. This observation leads to an easy algorithm to generate SSS. The following equations (from Koutsoyiannis, 2002) can be used to estimate the parameters ρ, φ and ξ:

$$\rho = 1.52 \, (H - 0.5)^{1.32} , \quad \varphi = 0.953 - 7.69 \, (1 - H)^{3.85} \tag{20}$$

$$\xi = \begin{cases} 0.932 + 0.087\,H & H \le 0.76 \\ 0.993 + 0.007\,H & H > 0.76 \end{cases} \tag{21}$$
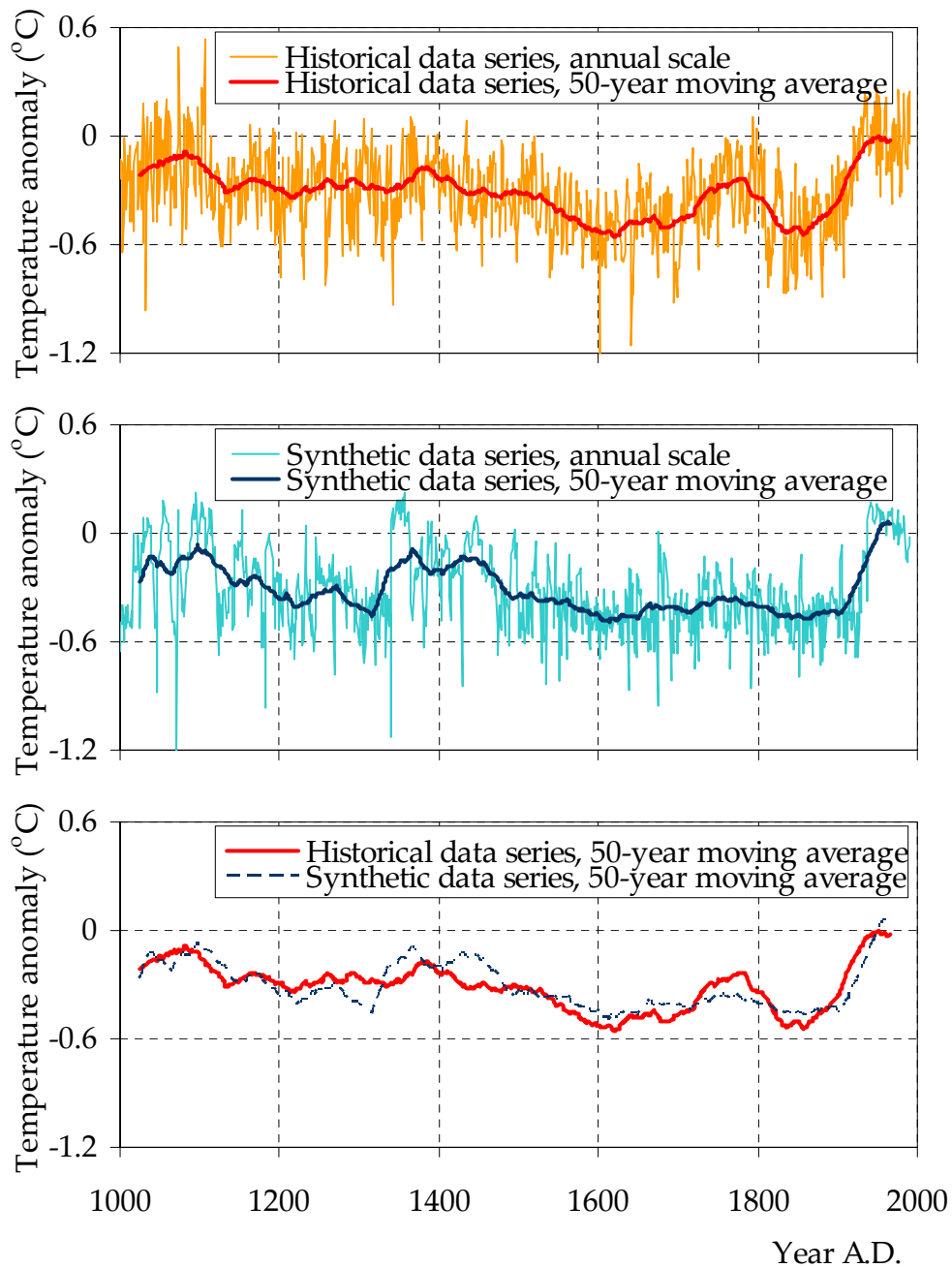
Figure 8 (Up) Plot of the Jones data series indicating the North Hemisphere temperature anomalies with reference to 1961–1990 mean; (middle) a synthetic time series generated by the double tent map fitted to the Jones data set and assuming $v = 4$; (down) comparison of the synthetic and original time series in terms of their 50-year moving averages.

The remaining parameters c_1 and c_2 can be then estimated such that the approximate autocorrelation function (17) match the exact function (5) for two lags, e.g. lags 1 and 100.

(Their values are obtained by solving two linear equations). Comparison plots of approximate autocorrelation functions based on equations (17) and (20)-(21) versus the exact SSS autocorrelation functions (equation (5)) for various values of the Hurst exponent H are shown in Figure 9. Equations (16) and (17) may be interpreted as representing the sum of three independent AR(1) processes, with lag one correlation coefficients ρ, φ, and ξ, and variances $(1 - c_1 - c_2)\gamma_0$, $c_1 \gamma_0$, and $c_2 \gamma_0$, respectively. Thus, the generation algorithm is as simple as the generation of three AR(1) series and their addition.
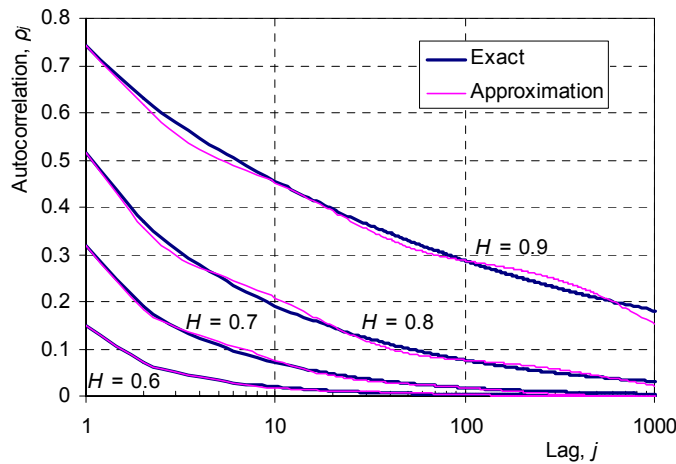
Figure 9 Approximate autocorrelation functions based on equations (17) and (20)-(21) vs. the exact SSS autocorrelation functions (equation (5)) for various values of the Hurst exponent H (from Koutsoyiannis, 2002).

The simple expressions of the statistics of the aggregated SSS process make possible a disaggregation approach for generating SSS (Koutsoyiannis, 2002). Specifically, let us assume that the desired length n of the synthetic series to be generated is 2^m where m is an integer (e.g., $n = 2, 4, 8, , \ldots$); if not, we can increase n to the next power of 2 and then discard the redundant generated items. We first generate the single value of $Z_1^{(n)}$ knowing its variance $n^{2H} \gamma_0$ (from (3)). Then we disaggregate $Z_1^{(n)}$ into two variables on the timescale $n/2$, i.e. $Z_1^{(n/2)}$ and $Z_2^{(n/2)}$ and we proceed this way until the series $Z_1^{(1)} \equiv X_1, \ldots, Z_n^{(1)} \equiv X_n$ is generated (see explanatory sketch in Figure 10).

We consider the generation step in which we disaggregate the higher-level amount $Z_i^{(k)}$ ($1 < i < n/k$) into two lower-level amounts $Z_{2i-1}^{(k/2)}$ and $Z_{2i}^{(k/2)}$ such that

$$Z_{2i-1}^{(k/2)} + Z_{2i}^{(k/2)} = Z_i^{(k)} \tag{22}$$

Thus, it suffices to generate $Z_{2i-1}^{(k/2)}$ and then obtain $Z_{2i}^{(k/2)}$ from (22). At this generation step we have available the already generated values of previous lower-level time steps, i.e., $Z_1^{(k/2)}$, …, $Z_{2i-2}^{(k/2)}$ and of next higher-level time steps, i.e., $Z_{i+1}^{(k)}$, …, $Z_{n/k}^{(k)}$ (see Figure 10). Theoretically, it is necessary to preserve the correlations of $Z_{2i-1}^{(k/2)}$ with all previous lower-level variables and all next higher-level variables. However, we can get a very good approximation if we consider correlations with only one higher-level time step behind and one ahead. Under this simplification, $Z_{2i-1}^{(k/2)}$ can be generated from the linear relationship

$$Z_{2i-1}^{(k/2)} = a_2 Z_{2i-3}^{(k/2)} + a_1 Z_{2i-2}^{(k/2)} + b_0 Z_i^{(k)} + b_1 Z_{i+1}^{(k)} + V \tag{23}$$

where a_2, a_1, b_0 and b_1 are parameters given by

$$\begin{bmatrix} a_2 \\ a_1 \\ b_0 \\ b_1 \end{bmatrix} = \begin{bmatrix} 1 & \rho_1 & \rho_2+\rho_3 & \rho_4+\rho_5 \\ \rho_1 & 1 & \rho_1+\rho_2 & \rho_3+\rho_4 \\ \rho_2+\rho_3 & \rho_1+\rho_2 & 2(1+\rho_1) & \rho_1+2\rho_2+\rho_3 \\ \rho_4+\rho_5 & \rho_3+\rho_4 & \rho_1+2\rho_2+\rho_3 & 2(1+\rho_1) \end{bmatrix}^{-1} \begin{bmatrix} \rho_2 \\ \rho_1 \\ 1+\rho_1 \\ \rho_2+\rho_3 \end{bmatrix} \tag{24}$$

with ρ_j given by (5), and V is an innovation with variance

$$\mathrm{Var}[V] = \gamma_0^{(k/2)} (1 - [\rho_2, \rho_1, 1+\rho_1, \rho_2+\rho_3]\,[a_2, a_1, b_0, b_1]^T) \tag{25}$$

where the superscript T denotes the transpose of a vector.

All parameters are independent of i and k and therefore they can be used in all steps. When $i = 1$ there are no previous time steps and thus the first two rows and columns of the above matrix and vectors are eliminated. Similarly, when $i = n / k$, there is no next time step and thus the last row and column of the above matrix and vectors are eliminated.

The power law of the power spectrum of SSS allows the generation of an SSS time series X_i filtering a series of white noise V_i by the symmetric moving average (SMA) scheme (Koutsoyiannis, 2000):

$$X_i = \sum_{j=-q}^{q} a_{|j|} V_{i+j} = a_q V_{i-q} + \ldots + a_1 V_{i-1} + a_0 V_i + a_1 V_{i+1} + \ldots + a_q V_{i+q} \tag{26}$$
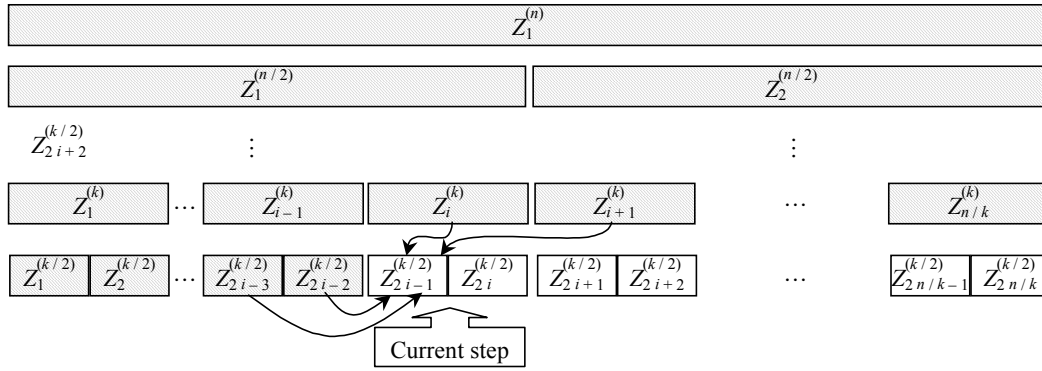
Figure 10 Explanation sketch of the disaggregation approach for generation of SSS. Grey boxes indicate random variables whose values have been already generated prior to the current step and arrows indicate the links to those of the generated variables that are considered in the current generation step (from Koutsoyiannis, 2002).

where q theoretically is infinity but in practice can be restricted to a finite number, as the sequence of weights a_j tends to zero for increasing j. Koutsoyiannis (2002) showed that the appropriate sequence of a_j is

$$a_j \approx \frac{\sqrt{(2 - 2H)\,\gamma_0}}{3 - 2H}\, \left(|j + 1|^{H + 0.5} + |j - 1|^{H + 0.5} - 2\,|j|^{H + 0.5}\right) \tag{27}$$

The sequence length q must be chosen at least equal to the desired number of autocorrelation coefficients m that are to be preserved. In addition, the ignored terms a_j beyond a_q must not exceed an acceptable tolerance $\beta\,\sigma$. These two conditions result in

$$q \ge \max\left[m, \left(\frac{2\,\beta}{H^2 - 0.25}\right)^{1 / (H - 1.5)}\right] \tag{28}$$

Thus, q can be very large (on the order of thousands to hundreds of thousands) if H is large (e.g. > 0.9) and β is small (e.g. < 0.001). Approximate autocorrelation functions based on equations (26) and (27) versus the exact SSS autocorrelation functions (equation (5)) for various values of H and q are shown in Figure 11.

This method can also generate non Gaussian series with skewness ξ_X by appropriately choosing the skewness of the white noise ξ_V. The relevant equations for the statistics of V_i, which are direct consequences of (26), are
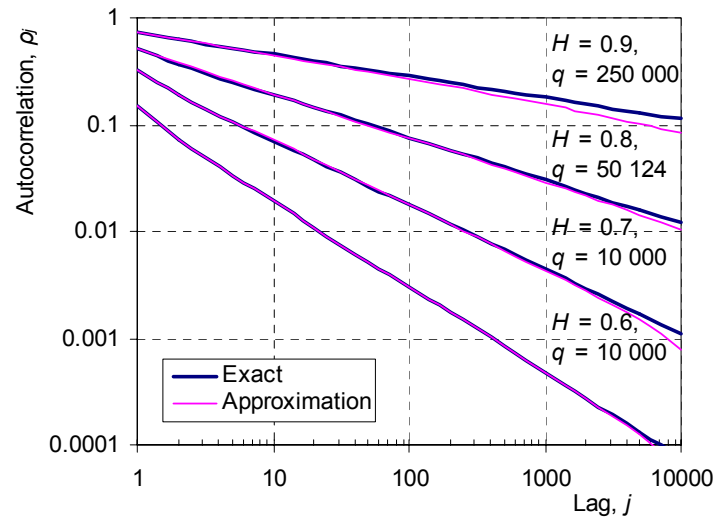
Figure 11 Approximate autocorrelation functions based on equations (26) and (27) vs. the exact SSS autocorrelation functions (equation (5)) for various values of the Hurst exponent H and of the number of weights q (from Koutsoyiannis, 2002).

$$\left(a_0 + 2\sum_{j=1}^{s} a_j\right) E[V_i] = \mu, \quad \text{Var}[V_i] = 1, \quad \left(a_0^3 + 2\sum_{j=1}^{q} a_j^3\right)\xi_V = \xi_X\, \gamma_0^{3/2} \tag{29}$$

Concluding remarks

More than half a century after its discovery, the Hurst phenomenon, has been verified to be almost omnipresent in several processes in nature (e.g. hydrology), technology (e.g. computer networks) and society (e.g. economics). However, still its consequences are not widely understood or are ignored; to quote Klemeš (1974), still it is regarded by many as "a ghost to be conjured away".

For example, in stochastic hydrological simulations that are used in hydrosystem modeling, the Hurst phenomenon is generally not reproduced. The most widespread stochastic hydrology packages, have not implemented any types of models that respect the Hurst phenomenon. However, today there exist methodologies, implemented into software packages, which can reproduce the Hurst phenomenon even in complicated situations, such as in multivariate setting with multiple timescales and asymmetric probability distributions (Koutsoyiannis, 2000; Koutsoyiannis and Efstratiadis, 2001; Langousis and Koutsoyiannis,

2003). In addition, as described above, the reproduction of the Hurst phenomenon in univariate problems is quite simple.

In hydrological analysis, it has been a common practice to detect falling or rising monotonic 'trends' in the available records, assume that these are deterministic components, and then 'subtract' them from the time series to obtain a 'detrended' time series, which is finally used in subsequent analyses. This common technique, which is described in several hydrological texts, is obviously a disrespect of the Hurst phenomenon. The 'trends' are in fact large scale fluctuations, i.e. the basis of the Hurst phenomenon. There could be regarded as deterministic components if a sound, physically-based model could capture them and also predict their evolution in the future. This, however, is not the case. The *a posteriori* fitting of a regression curve (e.g. a linear equation) on historical data series has no relation with deterministic modelling. The subtraction of the 'trends' from the time series results in a reduction of standard deviation, i.e. artificial decrease of uncertainty. This is exactly opposite to the real meaning of the Hurst phenomenon, which, as analyzed above, increases uncertainty substantially.

Even without adopting this 'detrending' technique, hydrological statistics, the branch of hydrology that deals with uncertainty, in its current state is not consistent with the Hurst phenomenon. Typical statistics used in hydrology such as means, variances, cross- and auto-correlations and Hurst coefficients, and the variability thereof, are based on classical statistical theory, which describe only a portion of natural variability and thus its results may underestimate dramatically the natural uncertainty and the implied risk.

The situation is even worse in climatology, which again uses the classical statistical framework but on longer timescales (e.g. 30 years). As demonstrated above, the consequences of the Hurst phenomenon in the natural variability increase as the timescale increases. Recently, many researchers are involved in the detection of anthropogenic climatic changes mostly using classical statistical tests, i.e. without taking into account the Hurst phenomenon. If statistical estimators respecting the Hurst phenomenon are used, which is a choice more consistent with nature, it is more unlikely that such tests will result in statistically significant changes.

Acknowledgment

References

Adenstedt, R. K. (1974), On large sample estimation for the mean of a stationary random sequence, *Ann. Statist.* 2, 1095–1107.

Beran, J. (1994), *Statistics for Long-Memory Processes*, vol. 61 of Monographs on Statistics and Applied Probability, Chapman and Hall, New York, USA.

Bhattacharya, R, N., Gupta, V. K. and Waymire, E. (1983) The Hurst effect under trends, *J. Appl. Prob.* 20, 649–662.

Bloomfield, P. (1992), Trends in global temperature, *Climatic Change* 21, 1–16.

Eltahir, E. A. B. (1996), El Niño and the natural variability in the flow of the Nile River, *Wat. Resour. Res.* 32(1), 131–137.

Evans, T. E. (1996), The effects of changes in the world hydrological cycle on availability of water resources. In: *Global Climate Change and Agricultural Production: Direct and Indirect Effects of Changing Hydrological, Pedological and Plant Physiological Processes* (ed. by F. Bazzaz and W. Sombroek), Chapter 2, FAO and John Wiley, Chichester, West Sussex, UK.

Haslett, J. and Raftery, A. E. (1989), Space–time modelling with long-memory dependence: assessing Ireland's wind power resource, *Appl. Statist.* 38(1), 1–50.

Hurst, H. E. (1951), Long term storage capacities of reservoirs, *Trans. ASCE*, 116, 776-808.

Jones, P. D., Briffa, K. R., Barnett, T. P. and Tett, S. F. B (1998a), Millennial Temperature Reconstructions. IGBP PAGES/World Data Center-A for Paleoclimatology Data Contribution Series #1998-039, NOAA/NGDC Paleoclimatology Program, Boulder, Colorado, USA (ftp.ngdc.noaa.gov/paleo/contributions_by_author/jones1998/)

Jones, P. D., Briffa, K. R., Barnett, T. P. and Tett, S. F. B. (1998b), High-resolution paleoclimatic records for the last millennium: interpretation, integration and comparison with General Circulation Model control-run temperatures, *Holocene* 8(4), 455–471.

Klemeš, V. (1974), The Hurst phenomenon: a puzzle? *Wat. Resour. Res.* 10(4), 675–688.

Klemeš, V. (1976), Geophysical time series and catastrophism, *Catastrophist Geology*, 1(1), 43-48.

Klemeš, V. (1978), Physically based stochastic hydrologic analysis, *Advances in Hydroscience*, 11, 285-356.

Klemeš, V., Sricanthan, R. and McMahon T.A. (1981), Long-memory flow models in reservoir analysis: What is their practical value? *Water Resources Research*, l7(3), 737-75l.

Koutsoyiannis, D. (2000), A generalized mathematical framework for stochastic simulation and forecast of hydrologic time series, *Water Resources Research,* 36(6), 1519-1533.

Koutsoyiannis, D. (2002), The Hurst phenomenon and fractional Gaussian noise made easy, *Hydrol. Sci. J.*, 47(4), 573-596.

Koutsoyiannis, D. (2003a), Climate change, the Hurst phenomenon, and hydrological statistics, *Hydrological Sciences Journal*, 48(1), 3-24.

Koutsoyiannis, D. (2003b), A toy model of climatic variability with scaling behaviour, *Hydrofractals '03, An international conference on fractals in hydrosciences*, Monte Verita, Ascona, Switzerland, August 2003, ETH Zurich, MIT, Université Pierre et Marie Curie (http://www.itia.ntua.gr/g/docinfo/585/).

Koutsoyiannis, D. (2003c), Hydrological statistics for engineering design in a varying climate, *EGS-AGU-EUG Joint Assembly, Geophysical Research Abstracts, Vol. 5*, Nice, April 2003, European Geophysical Society, American Geophysical Union (http://www.itia.ntua.gr/g/docinfo/565/).

Koutsoyiannis, D., and Efstratiadis, A. (2001), A stochastic hydrology framework for the management of multiple reservoir systems, *26th General Assembly of the European Geophysical Society, Geophysical Research Abstracts*, Vol. 3, Nice, March 2001, European Geophysical Society, (http://www.itia.ntua.gr/e/docinfo/54/).

Koutsoyiannis, D., and Efstratiadis, A. (2004), Climate change certainty versus climate uncertainty and inferences in hydrological studies and water resources management, *1st General Assembly of the European Geosciences Union, Geophysical Research Abstracts, Vol. 6*, Nice (http://www.itia.ntua.gr/g/docinfo/606/).

Langousis, A., and Koutsoyiannis, D. (2003), A stochastic methodology for generation of seasonal time series reproducing overyear scaling, *Hydrofractals '03, An international conference on fractals in hydrosciences*, Monte Verita, Ascona, Switzerland, August 2003, ETH Zurich, MIT, Université Pierre et Marie Curie (http://www.itia.ntua.gr/g/docinfo/586/).

Lasota, A., and Mackey, M.C. (1994), *Chaos, Fractals and* Noise*, Stochastic Aspects of Dynamics*, Springer-Verlag.

Mandelbrot, B. B. (1965), Une classe de processus stochastiques homothétiques a soi: application à la loi climatologique de H. E. Hurst, *C. R. Acad. Sci. Paris* 260, 3284–3277.

Mandelbrot, B. B. (1971), A fast fractional Gaussian noise generator, *Wat. Resour. Res.* 7(3), 543–553.

Mandelbrot, B. B. (1977), *The Fractal Geometry of Nature*, Freeman, New York, USA.

Mesa, O. J. and Poveda, G. (1993), The Hurst effect: the scale of fluctuation approach, *Wat. Resour. Res.* 29(12), 3995–4002.

Montanari, A., Rosso, R. and Taqqu, M. S. (1997), Fractionally differenced ARIMA models applied to hydrologic time series. *Wat. Resour. Res.* 33(5), 1035–1044.

Montanari, A., Taqqu, M.S. and Teverovsky, V. (1999), Estimating long-range dependence in the presence of periodicity: an empirical study. Mathematical and Computer Modeling, 29, 217-228.

National Research Council (Committee on Opportunities in the Hydrologic Sciences) (1991), *Opportunities in the Hydrologic Sciences*, National Academy Press, Washington DC, USA.

Radziejewski, M. and Kundzewicz, Z. W. (1997), Fractal analysis of flow of the river Warta, *J. Hydrol.* 200, 280–294.

Sakalauskienė, G. (2003), The Hurst Phenomenon in Hydrology, Environmental Research, Engineering and Management, 3(25), 16-20.

Salas, J. D. and Boes, D. C. (1980), Shifting level modelling of hydrologic time series, *Adv. Wat. Resour.* 3, 59–63.

Stephenson, D. B., Pavan, V. and Bojariu, R. (2000), Is the North Atlantic Oscillation a random walk? *Int. J. Clim.* 20, 1–18.

Toussoun, O. (1925), Mémoire sur l'histoire du Nil, in: *Mémoires a l'Institut d'Egypte*, vol. 18, 366–404.

Vanmarcke, E. (1983), *Random Fields*, The MIT Press, Cambridge, Massachusetts, USA.